JPG Journal of Petroleum Geology www.jpg.co.uk

Journal of Petroleum Geology, Vol. 42(1), January 2019, pp 79-90

EFFECT OF MICRITE CONTENT ON CALCITE CEMENTATION IN AN UPPER JURASSIC CARBONATE RESERVOIR, EASTERN SAUDI ARABIA

Shuo Zhang[a] and Peng Lu[b]*

Cementation is a primary factor reducing the porosity of carbonate rocks. It is a challenge to accurately model cementation for reservoir quality prediction because cementation is often a syndepositional process. In addition, cementation requires fluid flow to transport chemical species for precipitation within the pore spaces in a sediment. The development of fully-coupled depositional-hydrogeochemical models for cementation prediction is desirable, but the parameters which control the extent of cementation need to be identified and evaluated. This study uses petrographic data from 583 carbonate samples from 15 wells in an Upper Jurassic (Kimmeridgian) reservoir at a giant oilfield in eastern Saudi Arabia to investigate the controlling effects of micrite content on cementation in carbonate rocks. The results indicate that the amount of cement decreases with increasing micrite content in the carbonate rocks analysed. In addition, a modified Houseknecht method has been developed to assess the relative fractions of porosity reduction in carbonate sediments due to compaction and cementation. The method highlights variations in depositional porosity for different rock textures and distinguishes microporosity from interparticle porosity. In the studied samples, the total porosity loss due to compaction and cementation is generally less than 45%, and samples lose more porosity due to compaction than cementation. The relative importance of compaction and cementation in reducing porosity is different for different rock textures: wackestones and mudstones lose porosity mostly as a result of compaction, while grainstones, mud-lean packstones and packstones lose porosity due to both compaction and cementation.

INTRODUCTION

The accurate prediction of reservoir porosity and permeability is a key challenge in hydrocarbon exploration and recovery (Kupecz *et al.,* 1997). Current geological approaches to predict reservoir quality prior to drilling include both process-oriented geological models and purely empirical/statistical models (Ajdukiewicz and Lander, 2010). In mature areas where cores and logs are available to provide a calibration data set, statistical approaches may prove to be more effective. However, in undrilled basins or targets, theoretical relationships may need to be used. Reservoir property modelling of the effects of burial and compaction for sandstones has made considerable

[a] Aramco Research Center-Houston, 16300 Park Row Dr., Houston, TX, 77084, USA.
[b] EXPEC Advanced Research Center, Saudi Aramco, Dhahran, 31311, Saudi Arabia.

* Corresponding author, peng.lu@aramco.com

Key words: Reservoir quality prediction, Saudi Arabia, carbonate diagenesis, carbonate cementation, porosity loss, Houseknecht diagram, compaction.

progress with the development of Touchstone©/ Exemplar (Lander and Walderhaug, 1999; Walderhaug, 1996). This progress was facilitated by the availability of important data-sets which illustrate key elements in processes of sandstone compaction and cementation. The development of similar process-oriented models for carbonates is considerably more complex because of the reactivity of the sedimentary material, which may undergo syndepositional diagenesis (Kupecz *et al,*. 1997).

In sandstone reservoirs, *TouchStone*©, which is based on empirically-calculated compaction and precipitation rates of quartz cement, has proved to be a valuable predictive tool. The diagenetic history is modelled from the time of deposition to the present day. Compaction is modelled by an exponential decrease in intergranular volume as a function of effective stress. Quartz cementation is modelled as a precipitation-rate controlled process. The input data required for a simulation include the effective stress and temperature histories, together with the composition and texture of the modelled sandstones at the time of deposition. Burial history data may be obtained from basin models, while sandstone composition and texture are derived from point-count analyses of analogue thin sections. The appropriate compaction and quartz cementation parameters can be obtained from calibration studies.

The success of *TouchStone*© in sandstone reservoir quality prediction relies on the fact that the dominant primary pore type in sandstones is intergranular. Cementation by quartz and mechanical compaction will reduce pore sizes, but the pore type remains constant. The cementation rate is mostly limited by the intrinsic precipitation rate of quartz and not by the transport of dissolved silica. Carbonate diagenesis is more complicated than sandstone diagenesis due to the more rapid reaction kinetics of carbonate minerals (Kupecz *et al.,* 1997). Chemical reactions, fluid flow and deposition of carbonate sediments occur at comparable time scales and therefore cannot be decoupled. However, some aspects of carbonate porosity prediction may be modelled using the *TouchStone*© approach.

Carbonate diagenesis can be divided into early diagenesis (meteoric and marine) and later burial diagenesis. Numerous studies have shown that abundant cementation of carbonate rocks occurs during late burial diagenesis. Cathodoluminescence stratigraphy (e.g. Meyers and Lohmann, 1985) is a useful tool for identifying and correlating different generations of cement. Cathodoluminescence techniques have allowed researchers to correlate phases of cementation to geochemical environments (e.g. meteoric, marine, burial) and then to estimate the volumes of cement precipitated during the various diagenetic phases. Grover and Read (1983) concluded that major, but variable, cementation occurred under burial conditions in Middle Ordovician carbonates in Virginia (USA), with 3–45 vol.% of cement precipitated during shallow burial (< 3 km) and 50–95% during deep burial. Meyers and Lohmann (1985), in a study of Mississippian limestones in New Mexico, estimated that approximately 60% of the total cement was related to shallow-burial, marine phreatic processes, while approximately 40% was related to burial deeper than 1 km.

Brown (1997) examined porosity–depth relationships in the Madison Group (Mississippian) of the Williston Basin to investigate models of porosity loss in carbonates. The Williston Basin has a relatively simple burial history but there is considerable lateral variation in geothermal gradients across the basin, allowing porosity loss as a function of temperature to be studied. Brown (1997) divided the basin into areas of low, medium and high geothermal gradient, and then plotted average porosity versus depth for each area. The results indicated that higher temperatures generally result in lower carbonate porosity.

If porosity loss in carbonates is affected by temperature, it seems likely that the duration of thermal exposure may also play a role in modelling porosity loss. Schmoker (1984) demonstrated that carbonate porosity versus depth trends often follow a log-linear relationship between time and temperature. Brown (1997) also suggested that time should be considered when modelling carbonate porosity loss.

It appears, therefore, that various factors (temperature, time) used in modelling sandstone porosity loss may also be used in modelling porosity loss in carbonates. Perhaps the greatest difference for models of porosity loss in carbonates compared to siliciclastics may be that a thorough understanding of early diagenesis (pre-burial) is necessary to provide a template for models of the subsequent burial-related changes.

This paper presents a new data-set derived from petrographic data which investigates the relationship between micrite content and carbonate cementation in a Kimmeridgian carbonate reservoir in eastern Saudi Arabia. This data-set is evaluated in detail, and the implications for modelling various evolution stages of a carbonate pore system during burial are discussed. The relationships obtained may be used as a foundation for the development of models of carbonate cementation in the future.

METHODS AND MATERIALS

In this study, we attempt to evaluate the controls on carbonate cementation using petrographic data from 583 samples from 15 wells from a carbonate reservoir of Late Jurassic (Kimmeridgian) age in a giant oilfield

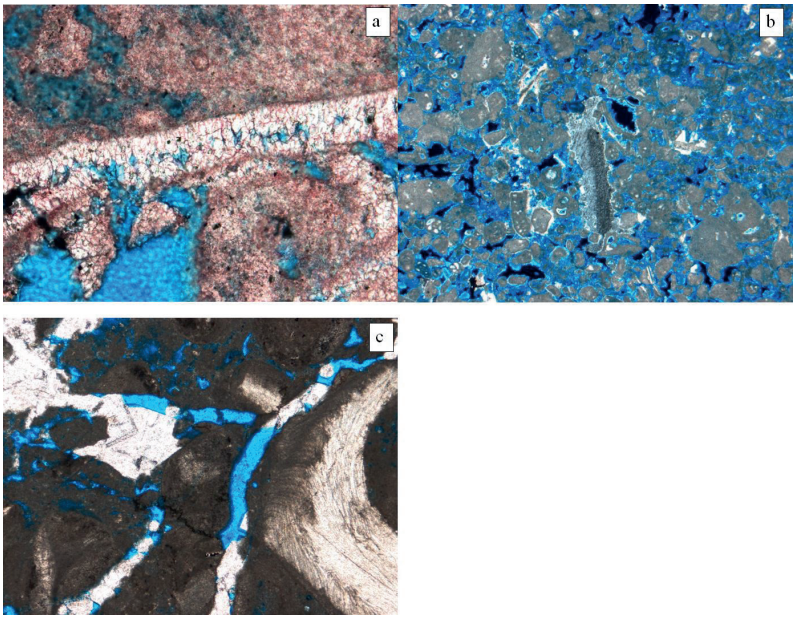

Fig. 1. Types of calcite cements observed in the studied reservoir rock including: (a) bladed cement forming isopachous rim; plane-polarized light (PPL), horizontal axis (HA) = 2.7 mm; (b) syntaxial overgrowth on an echinoderm fragment; cross-polarized light, HA = 8.5 mm; (c) equant calcite spar partially filling a set of fractures; note incipient dissolution of some of the grains resulting in the formation of minor secondary porosity; PPL, HA = 2.7 mm.

in eastern Saudi Arabia. The depositional environment of this reservoir is a homoclinal carbonate ramp (Lindsay *et al.*, 2006). Numerous studies have been focused on the structure, stratigraphy, depositional environment, lithofacies and diagenesis of the reservoir (e.g. Mitchell *et al.*, 1988; Meyer and Price, 1993; Handford *et al.*, 2002; Cantrell and Hagerty, 2003; Cantrell *et al.*, 2004; Swart *et al.*, 2005, 2016; Lindsay *et al.*, 2006; Lu and Cantrell, 2016). Zhang *et al.* (2018) used micrite content as a quantitative texture descriptor in multivariable regression and neural network models to predict permeability from porosity in the same reservoir. The uncertainty in permeability prediction was reduced from five to two orders of magnitude if micrite content was considered.

Thin sections were prepared from core plugs with a diameter of 1 in (2.54 cm). Standard helium porosity and air permeability (Klinkenberg corrected) measurements were conducted on horizontal and some vertical plugs. The thin sections were prepared following standard techniques, including vacuum impregnation with blue-dyed epoxy resin to allow porosity recognition. All the thin sections were uncovered and polished, and petrographic descriptions were made using a binocular petrographic microscope. Some thin sections (e.g. Figs 1a, 2c and 2d) were stained with Alizarin Red S and potassium ferricyanide for ferroan calcite identification (Dickson, 1965). All samples were classified according to their Dunham texture and their specific lithofacies classification (Mitchell *et al.*, 1988; Lindsay *et al.*, 2006). Porosity types were assigned according to the Choquette and Pray (1970) terminology.

The quantitative estimation of particle type, authigenic constituents, porosity and cement types was conducted by point counting. Between 400 and 600 points were counted along evenly-spaced traverses across or down the length of the thin sections using standard procedures (e.g. Kerr, 1977).

Counts of matrix, cements, grains, and pore space were made on a bulk basis. Cement is considered to be pore-filling material. Recrystallized grains or matrix were not counted as cement. The sum of grains, cements, matrix and porosity equals 100%. According to Folk (1962), particles less than 0.06 mm in diameter were defined as matrix. Percentages of porosity types were based on the amount of visible porosity. Microporosity was not distinguished. Specific grain types were identified because they are key indicators of depositional environments and were used to interpret the geologic framework of the reservoir rocks.

RESULTS

Cement types

$CaCO_3$ cements are usually classified according to their occurrence in different diagenetic environments. Four diagenetic zones can typically be defined in a gravity-governed sequence: (i) marine phreatic, (ii) mixing zone, (iii) meteoric phreatic and (iv) meteoric vadose from bottom to top of the sequence (Longmam, 1980; Tucker and Wright, 1990; Tucker, 1993).

$CaCO_3$ cements in the limestone samples analysed in this study are predominantly marine phreatic and meteoric phreatic. The marine phreatic realm begins at the seawater-sediment interface and may extend to

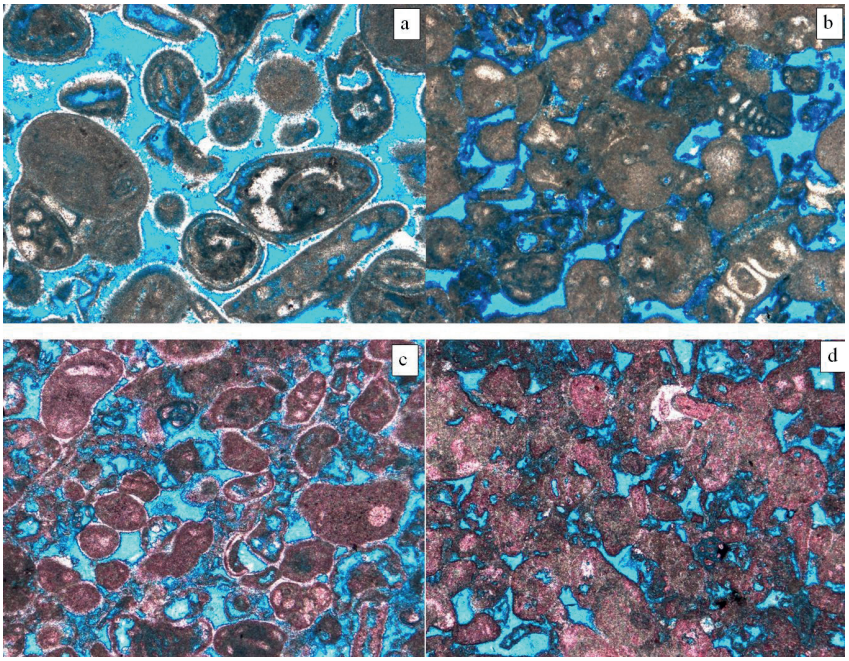

Fig. 2. Isopachous fibrous to bladed cement rim around grains precipitated relatively early in the diagenetic history of the Kimmeridgian limestones studied. While the cement may occlude some interparticle porosity, it may strengthen the framework structure and reduce the impact of later compaction in rocks with abundant isopachous rims (a, c) compared to their lightly cemented equivalents (b, d).

varying depths, depending on the seawater penetration. The realm is characterized by rock or sediment pores which are completely filled with normal marine water. The meteoric phreatic realm occurs on land below the groundwater table where pore spaces are filled by meteoric-sourced water. Other types of carbonate cement (such as vadose or deep burial cements) were not commonly observed in the studied reservoir rocks.

Marine phreatic cements occur primarily as isopachous fibrous to bladed crystals. This cement is common throughout grain-dominated facies and appears as a thin rim of 10 to 50 microns thickness that surrounds and separates individual grains (Fig. 1a). Although isopachous cement may occlude interparticle porosity, isopachous fibrous to bladed cement strengthens the rock fabric shortly after deposition, and thereby helps to preserve the original porosity by protecting the rock from later degradation by compaction or cementation (Mitchell *et al.*, 1988; Lindsay *et al.*, 2006). In the studied rocks, samples with extensive isopachous rims are generally less compacted than their non-cemented equivalents (compare, for example Figs 2a, c with Figs 2b, d).

Syntaxial calcite overgrowths are in general inclusion-rich and cloudy, but volumetrically insignificant. Therefore, they are likely to be of marine origin and were precipitated as high Mg calcite (HMC) initially (Lohmann and Meyers, 1977; Aissaoui, 1988; Durlet and Loreau, 1996).

Meteoric phreatic cements occur as clear, single crystal overgrowths (Fig. 1b) and as sparry equant calcite (Fig. 1c). Overall, meteoric cements are volumetrically minor in the carbonate samples studied and are only locally effective in occluding porosity.

The classification of marine or meteoric cements based on textural shapes and crystal relationships alone is open to debate. For a more reliable differentiation, isotopic and trace element analyses should be included (e.g. Meyers and Lohmann, 1985; Scholle and Ulmer-Scholle, 2003).

Amount of cement

In Fig. 3, the amount of cement is plotted against micrite content in the carbonate rocks studied. The micrite-free grainstones show the largest range of cementation, up to 20%. As the micrite content increases, the amount of cement decreases. For each micrite content value, there is a range of cement values. In an attempt to identify the factors that control the amount of cementation, the data-points in the cross-plot in Fig. 3a-d are grouped respectively by depositional facies, zone and texture and by the name of the field from which the samples were taken. Each depositional facies has a different range of values for micrite content and cement. For example, the skeletal-oolitic (SO) facies has low micrite content, mostly less than 5%, and a cement content ranging from 0 to 20%. The micritic (MIC) lithofacies has a wide range of micrite contents, from 10% to 90%, but barely contains any cement. There seems to be no clear distinction between groups when labelled by zone name or field name, i.e. the groups overlap with each other. The texture of the samples is mainly defined by micrite content following Dunham (1962), although we integrated porosity,

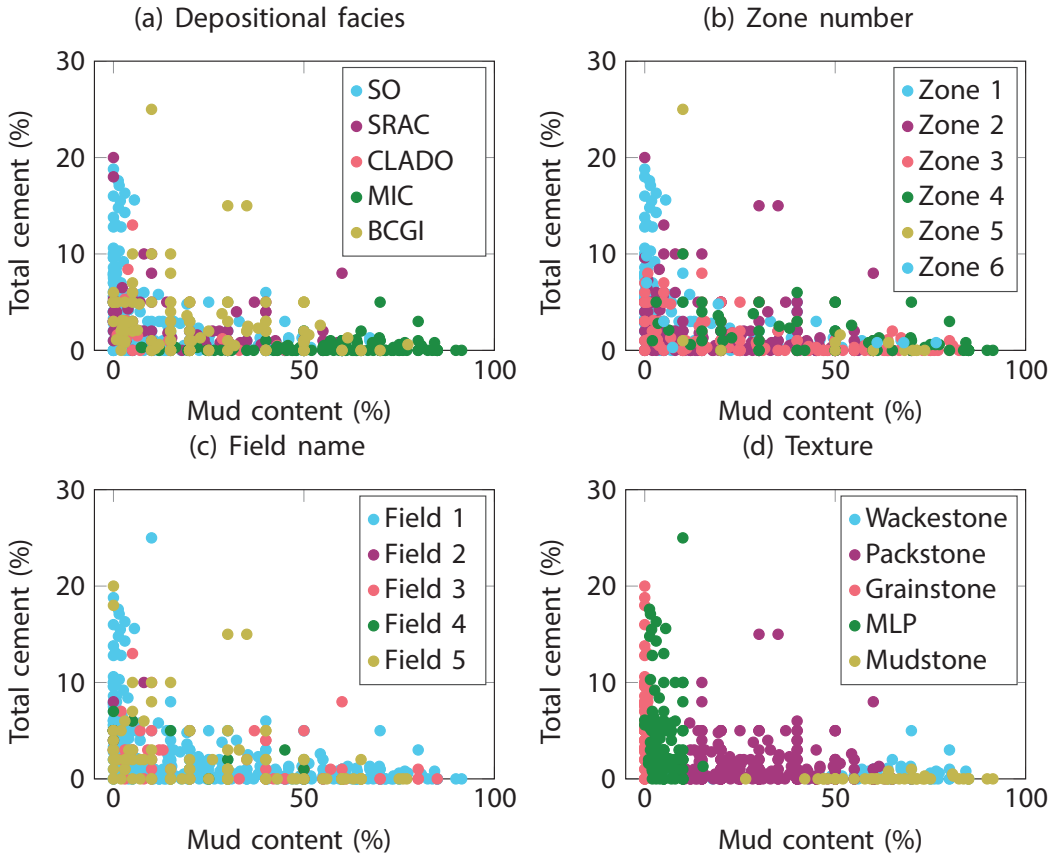

Fig. 3. The amount of total cement as a function of mud content grouped by depositional facies, zone, field name and texture. Carbonate lithofacies: SO: skeletal-oolitic; SRAC: stromatoporoid – red (green) algal – coral; CLADO: *Cladocoropsis*; MIC: micritic; BCGI: bivalve – coated grain – intraclast; MLP: mud-lean packstone.

permeability and core descriptions, in addition to thin section images, to facilitate the texture classification. Therefore, the boundaries between the groups in Fig. 3d largely but not fully coincide with the threshold micrite contents.

Different types of cement are plotted against micrite content in Fig. 4. Marine cement (fibrous to bladed isopachous) contributes most to the total cement, and correlates with micrite content in a pattern similar to the total cement. Equant cement, however, does not show a similar pattern. Equant cement can be as high as 10%, and is most abundant in bivalve-coated grain-intraclast (BCGI) limestones. The amount of syntaxial single crystals is less than 4% and is a minor component in the total cement.

DISCUSSION

A key observation in this investigation is that the amount of cement in the carbonate rocks studied decreases with increasing micrite content. Previous studies have shown that micrite content is a fundamental control on the porosity and permeability of depositional carbonate sediments (Enos and Sawatsky, 1981). This may provide an explanation for the relationship between cement and micrite content in present-day carbonate rocks.

Depositional porosity and permeability of carbonate sediments

Enos and Sawatsky (1981) reported the depositional porosities of Holocene carbonate sediments from Florida and Bahamas and related these to depositional textures. They found that the sediments with the highest micrite contents had the highest porosities. Micrite-free sediments, whose depositional texture corresponds to grainstone, had 40–50 % porosity. The porosities of grain-supported sediments containing some micrite (sedimentary equivalent of packstone) were 44–68 %. Using observations of depositional porosity and micrite content from their study, an empirical relationship between these variables was established (Fig. 5).

These authors also showed that porosity and permeability in Holocene carbonate sediments have a marked inverse relationship, which contrasts with the generally positive correlation in carbonate rocks. The inverse correlation between porosity and permeability in modern carbonate sediments probably occurs because a large fraction of porosity in micrite-rich sediments is microporosity. Enos and Sawatsky (1981) showed that if a simple model of filling intergranular pore space with micrite is adopted using the porosity values obtained from end-member lithologies, the expected porosities in sediments with increasing micrite fractions can be calculated. The observed

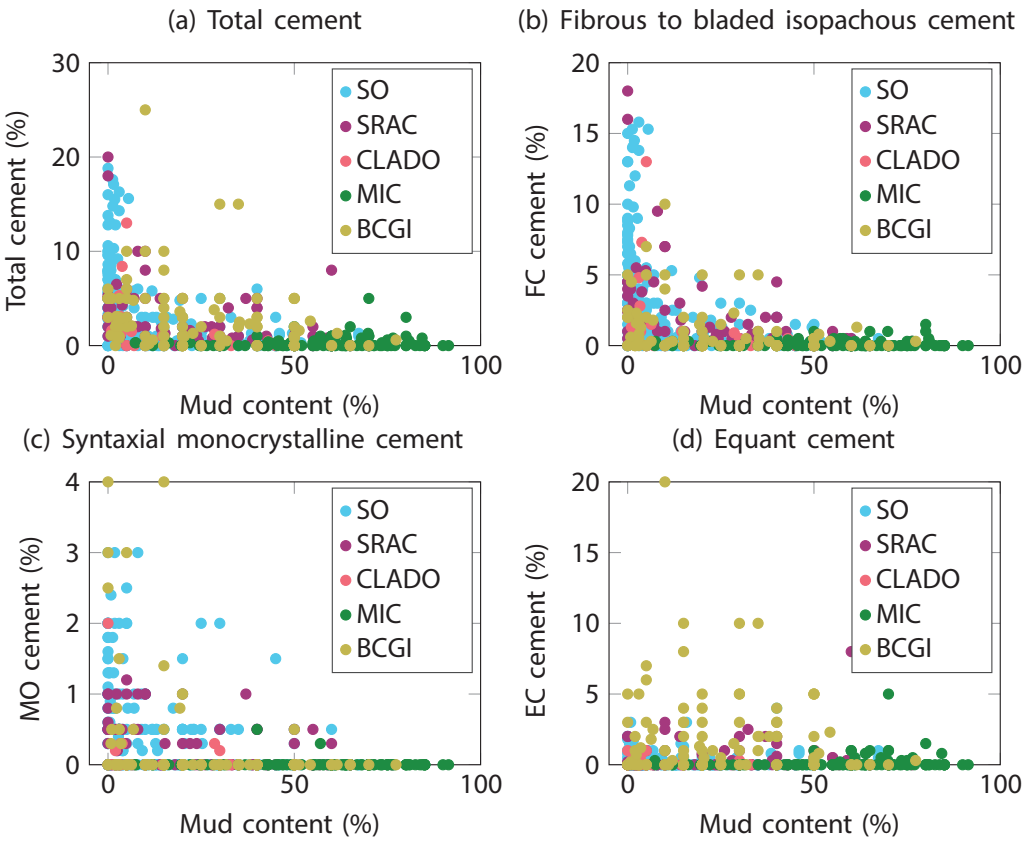

Fig. 4. The amount of total cement, fibrous to bladed isopachous (FC) cement, syntaxial monocrystalline (MO) cement, and equant (EC) cement as a function of mud content grouped by depositional facies. SO: skeletal-oolitic; SRAC: stromatoporoid – red (green) algal – coral; CLADO: *Cladocoropsis*; MIC: micritic, BCGI: bivalve – coated grain – intraclast.

porosity trend fits relatively well by assuming mixing of two-end members: grainstones with 45% porosity, and micrite with 80% microporosity.

Therefore, although the total porosity of carbonate sediments increases with increasing micrite content, the interparticle porosity decreases with micrite content. The decrease of cementation in carbonate rocks with increasing micrite content may therefore be due to two factors. The first is that there is less interparticle pore space in micrite-rich sediments for cements to grow; the other is that low interparticle porosity leads to low permeability of the carbonate sediments. The low permeability in micrite-rich sediments may then inhibit fluid flow and early cementation. In addition, in a submarine environment, the micrite content is an indication of hydraulic energy during deposition, which is lower for micrite-rich sediments and higher for grain-rich sediments. Lower hydraulic energy may correlate to a lower flow velocity of the fluid that reached the sediments, and thus a lower flux of materials for cementation. Overall, the micrite content affects the amount of cementation through the depositional interparticle porosity and the permeability of the sediments.

These relationships may have implications in forward depositional models where the amount of cement needs to be modelled. Cantrell *et al.* (2015) used *Sedsim* to reproduce the deposition of the Shu'aiba Formation in Saudi Arabia. The main assumption was that the duration of exposure above sea level was the fundamental control on both erosion and cementation associated with meteoric diagenesis. To simulate these processes, Cantrell *et al.* (2015) included empirical rules for erosion and porosity loss with cementation in their model. The erosion function was based on general experience in modern carbonates deposited in humid climatic settings; the effects of exposure were defined as erosion (removal of previously-deposited sediment) occurring within a certain period of time. In the Shu'aiba simulation, erosion was postulated to have begun after 10 ka of exposure, and to have proceeded at a rate of 1.5 cm/ka. Cements formed during subaerial exposure were also modelled as a function of time of exposure, starting from high initial depositional porosity to a time when all the porosity was completely occluded by cement after 8 Ma of exposure. Other diagenetic processes were not included in the model.

The observations in the present study show that the amount of cement in a carbonate rock is controlled by the micrite content of the sediments. Micrite-rich sediments tend to have lower depositional interpartical porosity and permeability, which then limits the fluid

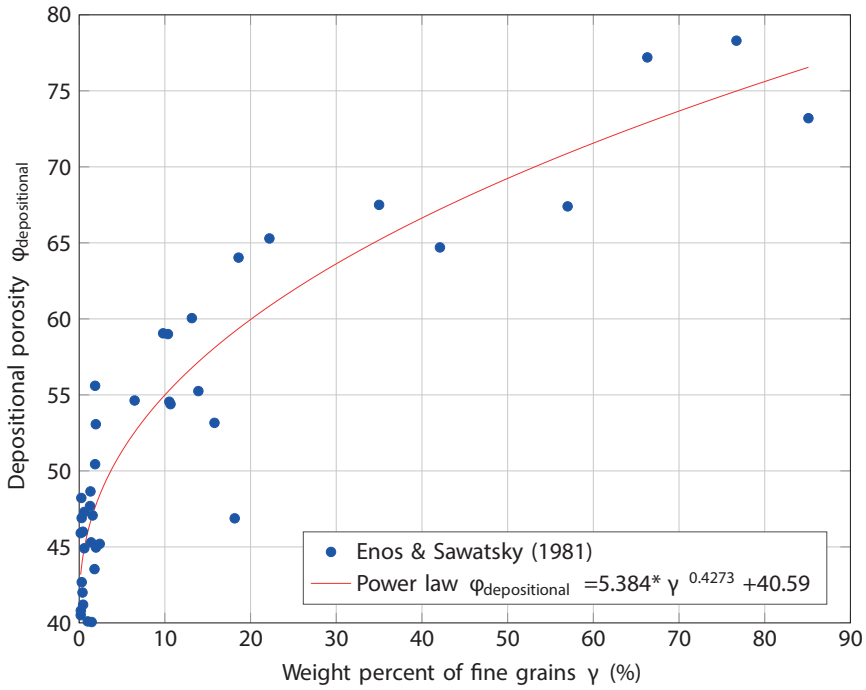

Fig. 5. Depositional porosity of modern carbonate sediments plotted against weight percent of fine grains (micrite), fitted with a power law function. Data from Enos and Sawatsky (1981).

flow required to transport chemical solutes needed for the cement to grow. This effect can be implemented in forward depositional models by defining a set of fuzzy rules for different lithofacies. At each time step, micrite content, or the ratio of fine to coarse grains, is an intermediate result from the depositional calculations. The fuzzy rules can be defined for the rates of cementation as a function of micrite content, reflecting its inhibiting role in cementation.

Relative importance of compaction and cementation in reducing porosity

When assessing the diagenetic modification of intergranular porosity, it is useful to separate the effects of compactional processes from the effects of cementation. Houseknecht (1987) presented a graphical technique with which the relative importance of compactional processes and cementation to porosity reduction can be quantified in clastic reservoirs. The vertical axis of the diagram represents intergranular volume, which is the sum of the intergranular porosity plus all the cements that occupy intergranular space; while the horizontal axis is cement content. An assumption made in this diagram is that the original porosity of depositional sand is 40%. The fraction of porosity reduction by compaction and cementation can thus be calculated in sandstones from the depositional porosity, the cementation volume, and the present-day intergranular porosity. Important improvements were made by Ehrenberg (1989), who incorporated the effects of bulk volume change during compaction on the compaction calculation; and Lundegard (1992), who introduced the COPL/CEPL (compaction porosity loss/cementation porosity loss) diagram. These methods work only when it is possible to assume a single value for depositional porosity for a given particle size distribution. In the present study, however, we have shown that the depositional interparticle porosity of carbonate sediments is also a function of micrite content in the sediments. Therefore, a modified approach is used to evaluate the relative fraction of porosity reduction by compaction and cementation in this study.

Before calculating the reduction of porosity by compaction and cementation, it is necessary to understand the fractions of different components in deposited carbonate sediments. Carbonate sediments can be considered as a combination of three components in volume: interparticle porosity (ϕ_i), micrite (M), and grains (G). Micrite consists of microporosity (ϕ_m) and micrite solids (M_s). The sum of interparticle porosity and microporosity within micrite is defined as the total depositional porosity (ϕ_d). Therefore

$$\phi_i + \phi_m + M_s + G = 100 \quad \text{(i)}$$

where $$\phi_i + \phi_m = \phi_d, \quad \text{(ii)}$$

and $$\phi_m + M_s = M. \quad \text{(iii)}$$

In Fig. 5, the depositional porosity of carbonate sediment can be calculated from the weight-percent of fine grains (micrite, γ). Two end-member values of depositional porosity can be determined. When the sediments consist only of grains ($\gamma = 0$), the depositional porosity is composed only of interparticle porosity, which is 40.59%. When the sediments are pure micrite ($\gamma = 1.0$), the value of the depositional porosity

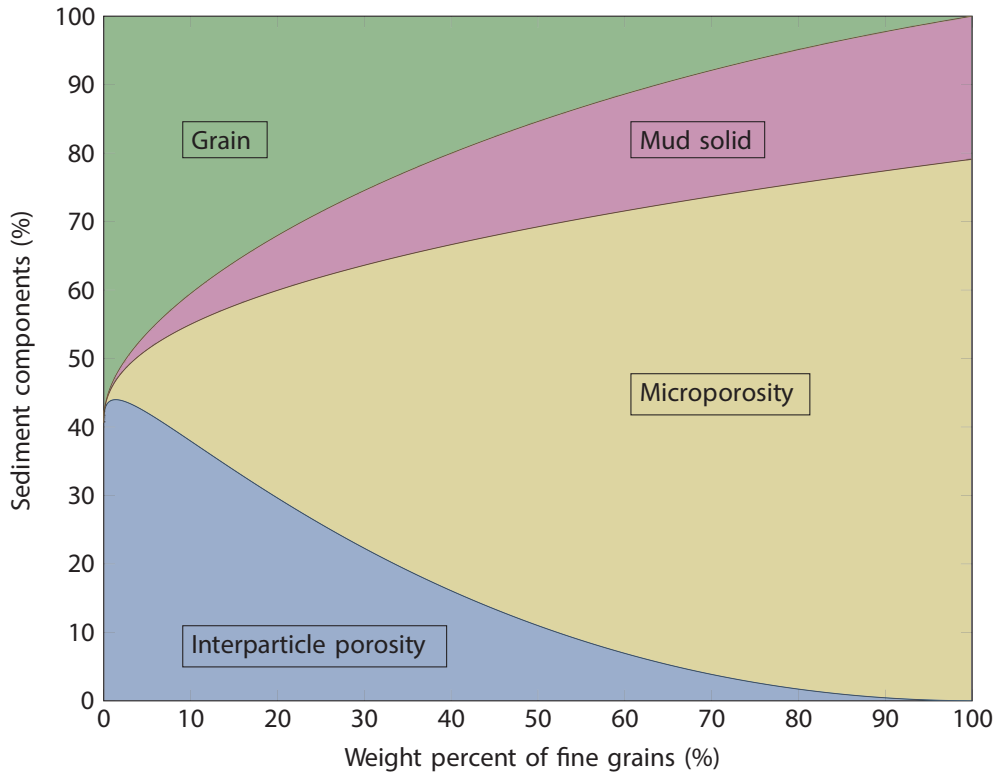

Fig. 6. Fractions of components in carbonate sediments as a function of weight-percent of fine grains (micrite).

(79.11%) is equal to the fraction of microporosity in micrite. Therefore, the fraction of microporosity in the bulk carbonate sediments is

$$\phi_m = 0.7911 \times M. \qquad \text{(iv)}$$

Note that microporosity mentioned in this study is a calculated value instead of a measured one, as the resolution of optical microscope is not sufficient to investigate microporosity.

In Fig.5, the depositional porosity is fitted against the weight-percent of micrite as follows:

$$\phi_d = 5.384 \times \gamma^{0.4273} + 40.59, \qquad \text{(v)}$$

where the weight-percent of micrite is defined as

$$\gamma = M_s / (M_s + G). \qquad \text{(vi)}$$

Combining Equations i, ii and vi, we obtain

$$M_s = \gamma (100 - \phi_d) \qquad \text{(vii)}$$

The range of γ is from 0 to 100%. For each γ value, the value of depositional porosity ϕ_d is first calculated using Eq. (v). The value of M_s is then calculated using Eq. (vii) with obtained γ and ϕ_d values. Finally, the value of G is calculated using Eq. (i). The results are presented in Fig. 6 where the bulk volume of carbonate sediments is divided into four components: interparticle porosity, microporosity, micrite solids, and grains. The sum of interparticle porosity and microporosity equals depositional porosity, and the sum of microporosity and micrite solids equals micrite content. Consistent with discussions in the previous section, interparticle porosity decreases with increasing micrite fraction although total porosity increases, because a larger fraction of the total porosity is microporosity for high micrite content samples.

The advantage of using weight-percent of micrite (γ) as the starting variable is that it does not change during compaction of carbonate sediments. Due to the change of bulk volume of carbonate sediments during compaction, the present micrite content, grain content and interparticle porosity are percentages of a different and smaller total rock volume compared to their depositional counterparts. However, the weight ratio of micrite to coarse grains does not change. Therefore, we can use the present weight percentage of micrite from point counting to calculate the fractions of sediment components during deposition.

We are aware of the possibility that some grains may be micritic, i.e. composed of micrite-like matrix. These grains may originally have been micritic, e.g. pellets, or may have been micritised after deposition. Our calculation assumes that all grains are sparitic and composed purely of solid material. In cases where some of the grains were originally micritic, grains must

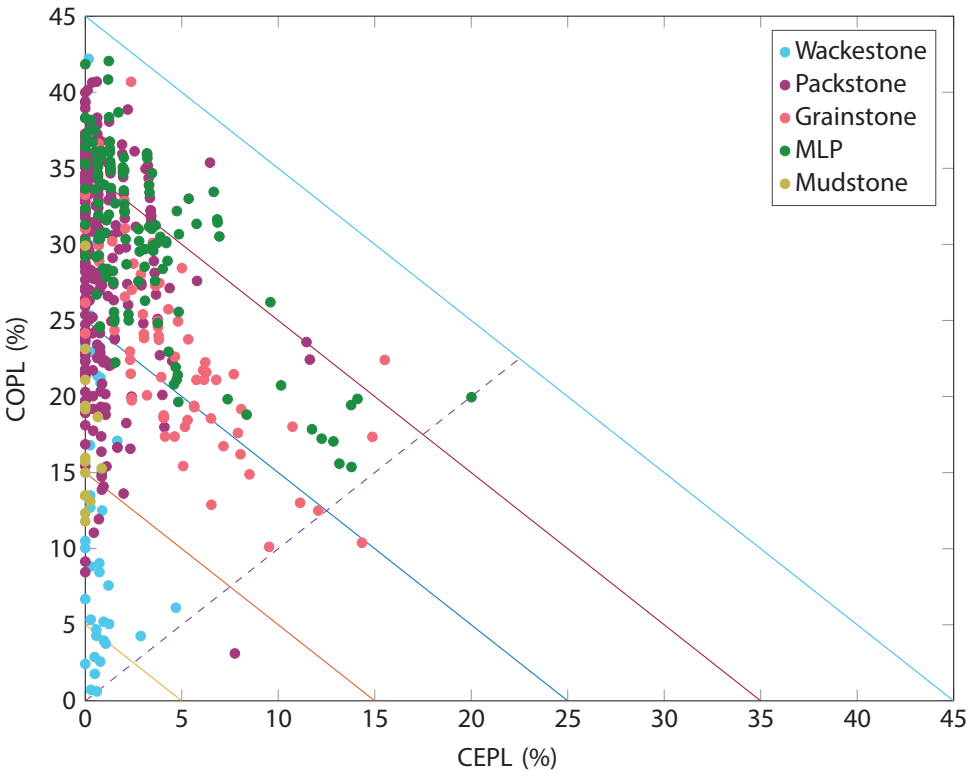

Fig. 7. Relative importance of porosity loss by compaction (COPL) and porosity loss by cementation (CEPL). MLP: mud-lean packstone. The dashed diagonal line separates samples in which compaction has been more important than cementation (upper left), from samples in which cementation has been more important than compaction (lower right) in determining intergranular porosity. The solid lines represent total porosity loss.

be separated into two fractions: a fraction of calcitic grains, and a fraction of micritic grains. However, the dataset in Enos and Sawatsky (1981) does not allow such a distinction to be made since the fractions of the different grains were not available.

With the depositional porosity calculated above, it is possible to follow the approach in Ehrenberg (1989) where the compaction porosity loss (COPL) is calculated as

$$COPL = \phi_i - \frac{(100 \times IGV - \phi_i \times IGV)}{(100 - IGV)} \qquad \text{(viii)}$$

where IGV is the present intergranular volume, and is calculated as the sum of the present interparticle porosity and the cement. In applying this formula, micrite is treated as part of the solid component, assuming that the volumes of micrite and grain do not change during compaction. The combined micrite and grain in this study is equivalent to the solid component in the Ehrenberg (1989) study.

The amount of original porosity destroyed by cementation (CEPL, cementation porosity loss) is calculated from the present volume-percent cement (CEM) as

$$CEPL = (\phi_i - COPL) \times \frac{CEM}{IGV} \qquad \text{(ix)}$$

Fig. 7 plots the calculated porosity loss due to compaction (COPL) against porosity loss due to cementation (CEPL). The dashed diagonal line on Fig. 7 separates samples in which compaction has been more important than cementation (upper left), from samples in which cementation has been more important than compaction (lower right). It can be observed that most samples lose more porosity by compaction than by cementation.

The relative importance of compaction and cementation in reducing porosity is different for different rock textures. Wackestones and mudstones lose porosity mostly by compaction, with the amount of total cement close to zero. Grainstones, mud-lean packstones and packstones lose porosity by both compaction and cementation. However, it seems that compaction has a larger effect on porosity loss compared to cementation in most samples, since they fall on the upper-left part of the diagram. The total porosity loss by compaction and cementation is in general less than 45% (the solid diagonal line in Fig. 7).

CONCLUSIONS

Petrographical point-counting of carbonate samples from a Kimmeridgian (Upper Jurassic) reservoir rock at a giant oilfield in eastern Saudi Arabia shows that the amount of early diagenetic cementation in carbonate rocks decreases with increasing micrite content. This control of micrite content on cementation needs to be incorporated in forward depositional models or other

models where porosity is reduced by cementation. The proposed approach in this study applies to modelling early cementation in carbonate sediments which is the major cement component in the studied reservoir. In reservoirs where late burial diagenesis is common, the amount of cement may be modelled using burial depth, temperature and time, possibly following a similar approach used in sandstone diagenesis prediction. The first step to model the change of porosity by cementation in carbonate rocks is to understand the depositional porosity and fractions of other components. We used the data reported in Enos and Sawatsky (1981) to develop a model that can be used to calculate the fractions of interparticle porosity, microporosity and grain content based on weight-fraction of micrite in depositional carbonate sediments. This serves as the starting point on which compaction and cementation can be applied in order to predict the final porosity of a carbonate rock.

A modified Houseknecht method is developed to assess the relative fractions of porosity reduction by compaction and cementation that is applicable to carbonate reservoir rocks. This modified approach uses the depositional porosities calculated from micrite content to evaluate the porosity loss during compaction and cementation. This approach has been used to evaluate the studied samples. The conclusion is that the total porosity loss by compaction and cementation is generally less than 45%, and most samples lose more porosity due to compaction than due to cementation.

ACKNOWLEDGEMENTS

The authors would like to thank Clemens Van Dijk, JPG reviewer Benoit Vincent (*Cambridge Carbonates)* and an anonymous referee for their insightful comments and suggestions during the reviewing process which significantly improved the clarity of the manuscript.

REFERENCES

AISSAOUI, D. M., 1988. Magnesian calcite cements and their diagenesis: dissolution and dolomitization, Mururoa Atoll. *Sedimentology*, **35**(5), 821-841.

AJDUKIEWICZ, J. M., and LANDER, R. H., 2010. Sandstone reservoir quality prediction: The state of the art. *AAPG Bulletin* **94**(8), 1083-1091.

BROWN, A., 1997. Porosity variation in carbonates as a function of depth: Mississippian Madison roup, Williston basin. In: J. A. Kupecz, J. Gluyas and S. Bloch (Eds), Reservoir quality prediction in sandstones and carbonates. *AAPG Memoir* **69**, 29-46.

CANTRELL, D., GRIFFITHS, C. and HUGHES, G., 2015. New tools and approaches in carbonate reservoir quality prediction: a case history from the Shu'aiba formation, Saudi Arabia. In: AGAR, S. M. and GEIGER, S. (Eds), Fundamental controls on fluid flow in carbonates: current workflows to emerging technologies. *Geol. Soc. Lond., Spec. Publ.* **406** (1), 401-425.

CANTRELL, D. L. and HAGERTY, R.M., 2003. Reservoir rock classification, Arab-D reservoir, Ghawar field, Saudi Arabia. *GeoArabia*, **8**, 435–462.

CANTRELL, D. L., SWART, P. K. and HAGERTY, R. M., 2004. Genesis and characterization of dolomite, Arab-D reservoir, Ghawar field, Saudi Arabia. *GeoArabia*, **9**, 11–36.

CHOQUETTE, P. W. and PRAY, L. C.,1970. Geologic nomenclature and classification of porosity in sedimentary carbonates. *AAPG Bulletin*, **54**, 207–250.

DICKSON, J. A. D., 1965. A modified staining technique for carbonates in thin section. *Nature*, **205**(4971), 587-587.

DURLET, C. and LOREAU, J. P., 1996. Inherent diagenetic sequence of hardgrounds resulting from marine ablation of exposure surfaces. Example of the Burgundy platform, Bajocian (France). *Comptes Rendus de l'Aacademie des Sciences Serie II fascicule A, Sciences de la Terre et des Planetes,* **323**(5), 389-396.

EHRENBERG, S., 1989. Assessing the relative importance of compaction processes and cementation to reduction of porosity in sandstones: Discussion; compaction and porosity evolution of Pliocene sandstones, Ventura basin, California: Discussion. *AAPG Bulletin* **73** (10), 1274-1276.

ENOS, P. and SAWATSKY, L., 1981. Pore networks in Holocene carbonate sediments. *Journal of Sedimentary Research* **51** (3) 961-985.

FOLK, R. L., 1962. Spectral subdivision of limestone types. In: Ham, W.E. (Ed.), Classification of carbonate Rocks – A Symposium. *AAPG Memoir* **1**, 62-84.

GROVER Jr, G. and READ, J., 1983. Paleoaquifer and deep burial related cements defined by regional cathodoluminescent patterns, middle Ordovician carbonates, Virginia. *AAPG Bulletin* **67** (8), 1275-1303.

HANFORD, C.R., CANTRELL, D.L. and KEITH, T. H., 2002. Regional facies relationships and sequence stratigraphy of a super-giant reservoir (Arab-D Member), Saudi Arabia. In: Armentrout, J.M. (Ed.), Sequence Stratigraphic Models for Exploration and Production: Evolving Methodology, Emerging Models and Application Histories. 22nd Annual Bob F. Perkins Research Conference. Gulf Coast Section SEPM (GCSSEPM), Houston, TX, 539–564.

HOUSEKNECHT, D.W., 1987. Assessing the relative importance of compaction processes and cementation to reduction of porosity in sandstones. *AAPG Bulletin* **71** (6), 633-642.

KERR, P. F., 1977. Optical Mineralogy. 4th Ed., McGraw-Hill, New York 492 pp.

KUPECZ, J. A., GLUYAS, J. and BLOCH, S., 1997. Reservoir quality prediction in sandstones and carbonates: An overview. In: Kupecz, J. A., Gluyas, J. and Bloch, S. (Eds), Reservoir Quality Prediction in Sandstones and Carbonates. *AAPG Memoir,* **69**, vii-xxiv.

LANDER, R. H. and WALDERHAUG, O., 1999. Predicting porosity through simulating sandstone compaction and quartz cementation. *AAPG Bulletin* **83** (3), 433-449.

LINDSAY, R. F., CANTRELL, D. L., HUGHES, G. W., KEITH, T. H., MUELLER, H. W., and RUSSELL, S. D., 2006. Ghawar Arab-D reservoir: widespread porosity in shoaling-upward carbonate cycles, Saudi Arabia. In: Giant Hydrocarbon Reservoirs of the World: From Rocks to Reservoir Characterization and Modelling. P. M. Harris and L. J. Weber (Eds), *AAPG Memoir* **88** / *SEPM Special Publication*, 97-137.

LOHMANN K. C. and MEYERS, W. J., 1977. Microdolomite inclusions in cloudy prismatic calcites; a proposed criterion for former high-magnesium calcites. *Journal of Sedimentary Research*, **47**(3), 1078-1088.

LONGMAN, M. W., 1980. Carbonate diagenetic textures from nearsurface diagenetic environments. *AAPG Bulletin*, **64**, 4, 461-487.

LUNDEGARD, P. D., 1992. Sandstone porosity loss: a "big picture" view of the importance of compaction. *Journal of Sedimentary Research*, **62** (2), 250-260.

LU, P. and CANTRELL, D., 2016. Reactive Transport Modelling of Reflux Dolomitization in the Arab-D Reservoir, Ghawar Field, Saudi Arabia. *Sedimentology*, **63**, 865-892.

MEYER, F. O. and PRICE, R. C., 1993. A new Arab-D depositional model, Ghawar field, Saudi Arabia. *SPE Paper* 25576 presented at the Middle East Oil Show, 3-6 April 1993, Bahrain.

MEYERS, W. J. and LOHMANN, K. C., 1985. Isotopic geochemistry of regionally extensive calcite cement zones and marine components in Mississippian limestones, New Mexico: In: Carbonate Cements. N. Schneiderman and P. Harris (Eds), Society of Economic. Paleontologists and Mineralogists, *Special Publication*, **36**, 223-240.

MITCHELL, J. C., LEHMANN, P. J., CANTRELL, D. L., AL-JALLAL, I. A. and Al-THAGAFY, M. A. R., 1988. Lithofacies, diagenesis and depositional sequence; Arab-D Member, Ghawar field, Saudi Arabia. In: Giant Oil and Gas Fields – A Core Workshop. A. J. Lomando and P. M. Harris (Eds), *Soc. Econ. Paleont. Mineral Core Workshop*, **12,** 459-514.

SCHMOKER, J. W., 1984. Empirical relation between carbonate porosity and thermal maturity: An approach to regional porosity prediction. *AAPG Bulletin* **68** (11), 1697-1703.

SCHOLLE, P. A. and ULMER-SCHOLLE, D. S., 2003. A Color Guide to the Petrography of Carbonate Rocks: Grains, Textures, Porosity, Diagenesis. *AAPG Memoir* **77**.

SWART, P. K., CANTRELL, D. L., WESTPHAL, H., HANDFORD, C. R. and KENDALL, C. 2005. Origin of dolomite from Ghawar field, Saudi Arabia: evidence from petrographic and geochemical constraints. *Journal of Sedimentary Petrology*, **75**, 476491.

SWART, P. K., CANTRELL, D. L., ARIENZO, M. M. and MURRAY, S. T., 2016. Evidence for high temperature and ^{18}O-enriched fluids in the Arab-D of the Ghawar Field, Saudi Arabia. *Sedimentology*, **63**, 1739-1752.

TUCKER, M. E. and WRIGHT, V. P., 1990. Carbonate Sedimentology. Blackwell, Oxford, 482 pp. doi.org/10.1002/9781444431417.

TUCKER, M. E., 1993. Carbonate diagenesis and sequence stratigraphy. In: V.P. Wright (Ed.), Sedimentology Review, Blackwells, Oxford, pp. 51-72.

WALDERHAUG, O., 1996. Kinetic modelling of quartz cementation and porosity loss in deeply buried sandstone reservoirs. *AAPG Bulletin* **80** (5), 731-745.

ZHANG, S., LU, P., CANTRELL, D., ZARETSKIY, Y., JOBE, D. and AGAR, S. M., 2018. Improved quantification of the porosity – permeability relationship of limestones using petrographical texture. *Petroleum Geoscience,* **24**, 440-448. doi.org/10.1144/petgeo2017-052.